Channel models, samples and network deployment strategies

Aymen Jaziri, Yoann Corre, Jean-Baptiste Doré, David Demmer, Rafik Zayani

Funded by:
anr
Supported by:
ir
Images & Réseaux

Grant agreement ANR-22-CE25-0015

Deliverable D1.2

Channel models, samples and network deployment strategies

Delivery date	01/09/2024
Version	0.0
Editor	Aymen Jaziri, Yoann Corre – SIRADEL
Authors	Aymen Jaziri, Yoann Corre – SIRADEL Jean-Baptiste Doré, David Demmer, Rafik Zayani – CEA Leti
Dissemination	Public

History

Version	Date	Modification	Author(s)
1.0	01/09/2024	First version	See above

Executive summary

This document details the creation of a radio channel database using digital twin. The provided database will be exploited through the other work packages in order to optimize algorithms and improve the performance of the studied cell-free mMIMO technology.

An automated calculation chain is employed to generate a substantial volume of data samples. The calibration phase ensures that the generated data aligns with real-world conditions and expectations. Following calibration, the generation phase involves the deterministic simulation of MIMO links. Then, the data samples undergo a compression phase. This involves the use of advanced algorithms to reduce the size of the data without loss of information, ensuring efficient storage and processing.

Once the data samples are prepared, an initial analysis is conducted. This analysis primarily focuses on propagation-related metrics, which are crucial in understanding the performance and effectiveness of the network designs. These metrics include the distribution of received power, optical visibility, and overlapping indicators. By analysing these metrics, we can gain valuable insights into the network's performance under various conditions. This initial analysis serves as a foundation for more detailed and technology-specific evaluations in the future.

Table of content

List of Acronyms

5G	5th Generation
5G-NR	5G New Radio
BS	Base Station
AP	Access Point
SAP	Small AP
MAP	Macro AP
UE	User Equipment
AE	Antenna Element
MIMO	Multiple Input Multiple Output
mMIMO	Massive MIMO
CF mMIMO	Cell-Free mMIMO
AVG	Automated Guided Vehicles
RB	Resource Block
TDL	Tapped Delay Line
CSV	Comma Separated Values
Tx	Transmitter
Rx	Receiver
RMSE	Root Mean Square Error
XPR	Cross-Polarization Ratio
LOS	Line Of Sight
NLOS	Non LOS
SISO	Single Input Single Output
CDF	Cumulative Ditribution Power
RSRP	Reference signal received power

1 Introduction

This document outlines the creation of an extensive radio channel database, specifically designed to support WP3 studies, particularly those employing learning methodologies. The database is populated with realistic data derived from the digital twins of urban and factory environments. The channel samples provided are pivotal in enhancing the CF-mMIMO system and facilitating precise performance evaluations of the same.

Initially, we detail the scenarios, chosen deployment strategies (primarily the positioning of potential sites and the type of antenna to be utilized), the configuration of radio parameters, and the spatial distribution of User Equipment (UEs) within the scene. Subsequently, we suggest a series of network designs (deployments) that serve as a common foundation for all POSEIDON partners to validate methodologies and assess the performance of each partner's contribution.

In the second segment of the document, we delineate and assess the performance of an automated, time-optimized calculation chain. This chain is used to emulate a substantial volume of data samples and compress it with minimal degradation. Our methodology includes the deterministic simulation of MIMO broadband links and the Tapped Delay Line (TDL) model [2], spanning various network deployment candidates (including cellular mMIMO and CF-mMIMO) and incorporating time (via mobility models) and frequency (via fading) variations. The advantages for POSEIDON stem from the genuine multi-AP spatial and temporal consistency offered by ray-tracing, and the generation of fading properties unique to each deployment under consideration.

Lastly, we present initial analysis using the channel samples for the proposed network designs. This analysis includes mainly propagation-related metrics such as received power distribution, optical visibility and overlapping indicators.

2 Scenarios for ray-tracing channel predictions

2.1 Urban scenarios for public networks

2.1.1 Study areas

We selected two dense urban areas in Paris in order propose new solutions (algorithms, mechanisms) for a more efficient, robust and scalable CF-mMIMO technology.

Figure 1 and Figure 2 show the 3D map data model of the two study areas. The first area is next to "Gare du Nord"; its size is 0.15 km². The second area is in "Les Halles" (touristic and commercial zone); its size is 0.41 km².

In the rest of the document, we refer to the first area as **UA1** for urban area 1 and **UA2** for the second urban area.

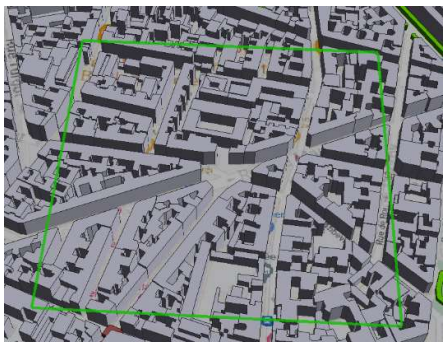

Figure 1 – 3D environment modelling of the study area UA1

Figure 2 – 3D environment modelling of the study area UA2

2.1.2 Network sites candidates

The scenarios for channel prediction have been selected so that they can support the evaluation of different network layers/technologies:

- Cellular mMIMO BSs operating at 3.5 GHz (the reference configuration to evaluate the gains/losses of CF-mMIMO technology): There are 8 Base Stations (BS) pointing to UA1 and 9 BSs pointing to UA2. As explained in [1], the cellular mMIMO network is inspired from an existing 5G deployment by a French mobile network operator. The regulator's website www.cartoradio.fr allows extracting information about the deployed radio access technology, frequency, GPS position, height, and azimuths.

- CF-mMIMO Macro APs (MAP) operating at 6 GHz: For MAPs, we consider the same positions used for the cellular mMIMO as it might be of interest to place MAPs on top of high buildings in a heterogeneous CF-mMIMO network.

- CF-mMIMO omnidirectional Small APs (SAP) operating at 6 GHz: SAPs are placed on lampposts while considering an inter-site distance equal to 50m. Therefore, we consider 27 SAPs for UA1 and 87 SAPs for UA2.

- CF-mMIMO directive SAPs operating at 6 GHz: For directive SAPs, we consider the same positions as the omnidirectional SAPs but in each site we perform sectorization to point to different directions of the streets.

Figure 3 and Figure 4 depict the macro and small-cell antennas in UA1 and UA2, respectively.

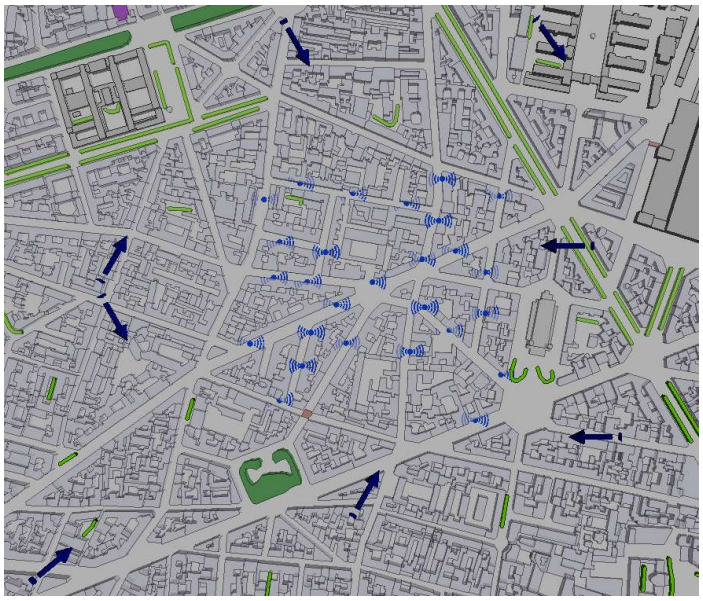

Figure 3 – Network infrastructure (AP candidates) in UA1

Figure 4 – Network infrastructure (AP candidates) in UA2

Table 1 summarizes the important BS/AP parameters that we consider in the channel predictions.

Table 1: Parameters configuration for urban BS/AP

<table>
<tr><th rowspan="2">Parameter</th><th colspan="4">Value</th></tr>
<tr><th>Cellular</th><th>MAP</th><th colspan="2">SAP</th></tr>
<tr><td rowspan="2">Spectrum</td><td>3.5 GHz / 100 MHz</td><td>6 GHz / 100 MHz</td><td colspan="2">6 GHz / 100 MHz</td></tr>
<tr><td colspan="4">Target frequency resolution = 1 RB = 12*15*2^μ kHz = 360 kHz➔ #RBs = 273
With μ refers to the numerology which is equal to 1</td></tr>
<tr><td>BS/AP configuration</td><td colspan="2">Height: from Cartoradio (real data)
Sectorization: from Cartoradio
Prediction radius: 1000m</td><td colspan="2">Height: 10m
Density: 1 site every 50m
Sectorization: tri or omni
Prediction radius: 200m</td></tr>
<tr><td>BS/AP antenna</td><td colspan="2">128 antenna elements (AE): 8x8x2
Dual-polar (+/-45°)
Planar vertical antenna array with separation λ/2
Beamwidth per AE: H95°, V95°
Gain per AE: 6.8 dBi</td><td>Omni
128 AEs: 4x4x4x2
Dual-polar (V/H)
Cubic antenna array with separation λ/2
Radiation pattern per AE: omni
Gain per AE: 6 dBi</td><td>Tri
128 AEs: 8x8x2
Dual-polar (V/H)
Planar vertical antenna array with separation λ/2
Beamwidth per AE: H95°, V95°
Gain per AE: 6.8 dBi</td></tr>
</table>

The proposed antenna configuration (especially the cubic antenna array) is only used for channel data generation as it must cover all the possible antenna configurations that we may study during the project. A specific simulation study will use a subset of the predicted antenna elements, for instance to investigate linear array or rectangular arrays. So the channel database is accompanied with an extraction function that permits to set a particular BS antenna configuration.

2.1.3 Data traffic distribution

The two considered scenarios have different spatial data traffic characteristics.

In UA1, the UEs are uniformly distributed following a density of 8400 UEs/km². 80% of UEs are indoor and located in different buildings' floors and 20% of UEs are located outdoors. The total number of UEs generated in UA1 is 1315. Figure 5 depicts the positions of the UEs in UA1.

Figure 5 – Spatial distribution of data traffic UEs in UA1

In UA2, we have the same density of UEs. However, we consider a non-uniform distribution due to the presence of hotspots (high number of connected users) e.g. near the shopping mall, in the park and close to the museum. Half of the generated UEs are indoor. The total number of UEs considered in this scenario is 5932. Figure 6 depicts the positions of the UEs in the scene.

Figure 6 – Spatial distribution of data traffic UEs in UA2

The UEs parameters including antenna parameters are summarized in Table 2.

Table 2: Parameters configuration for UEs

Parameter	Value
UE configuration	Height: 1.5m Density: 8400 UEs/km²
UE antenna	4 AEs Dual-polar (V/H) 2x1 horizontal linear array with separation λ/2 Radiation pattern per AE: isotropic Gain per AE: 0 dBi

It is worth noting that the set of generated UEs is not expected to correspond to the set of UEs active at a given time slot. Number of generated UEs is much higher than the expected number of active UEs. The objective is to construct and share a consistent database of samples. From this database, various scenarios can be experimented: random UE selections (as for Monte-Carlo simulations), various antenna configurations, and different AP densities. This method provides us with the flexibility to simulate a wide range of scenarios and network conditions.

2.1.4 Mobility (vehicular)

For urban mobility, we interfaced Siradel software with an external tool (SUMO [3]). SUMO is an open source software tool for modelling vehicle traffic, including public transport and pedestrians. Developed by the German Research Center for Artificial Intelligence (DFKI), it is most often used for research projects, traffic studies and the development of traffic management strategies, and has the capacity to simulate transport networks on the scale of a city (see Figure 7). It features multi-method traffic generation, performance evaluation and an API for integration and extension to other tools.

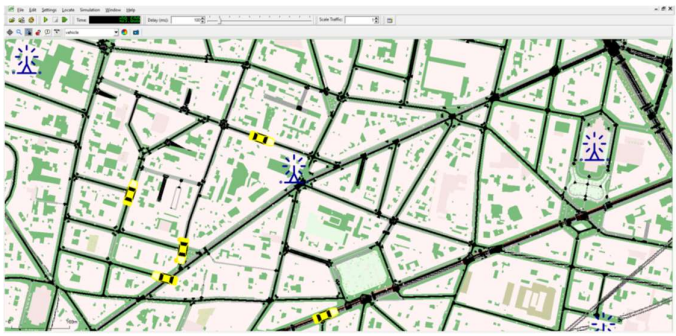

Figure 7 – SUMO GUI for urban mobility simulation

We propose two different scenarios:

- VA1: Few vehicles (around 10) travelling in UA1 for a small period of time (1 second) with resolution of 1 ms.
- VA2: Few vehicles (around 10) travelling in UA1 for a longer period of time (60 seconds) with resolution of 100 ms.

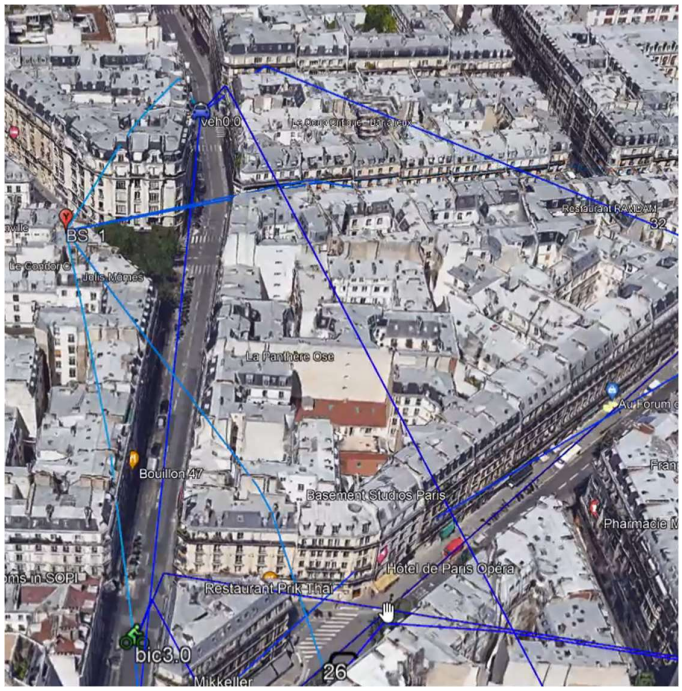

Figure 8 – Illustration of the signal propagation within urban mobility scenarios in Google Earth

Throughout the course of the project, we will be examining diverse scenarios and configurations. We have chosen to study mobility scenarios in a best-effort mode, given that the impact of mobility is not the primary focus of this project. This approach allows us to allocate our resources and attention effectively towards the main objectives of the project.

2.1.5 Selected network designs

With the considered candidate APs, there can be various possible network designs to be studied. Each researcher/partner in POSEIDON can optimize its algorithms and solutions based a specific design. Nevertheless, we decided to validate our different contributions and evaluate the efficiency of our propositions using a common set of network deployments.

2.1.5.1 UA1 selected designs:

For UA1, we selected 9 network designs. We aim to study the impact of variating the APs density and the use of directive antennas versus omnidirectional ones. Table 3 summarizes the number of APs per design.

Table 3: Summary of selected network designs for UA1

Network design	UA1_1 (benchmark configuration)	UA1_2 UA1_2bis	UA1_3 UA1_3bis	UA1_4 UA1_4bis	UA1_5 UA1_5bis
#APs		8 MAP +10SAP omni	8 MAP+12SAP omni	8 MAP+17SAP omni	8 MAP+8SAP omni+19 SAP directive
#BSs/APs	8 BS	8 BS +10SAP omni	8 BS+12SAP omni	8 BS+17SAP omni	8 BS+8SAP omni+19 SAP directive

UA1_1 represents a cellular selected design, useful for benchmarking the new proposed system, as we aim to compare the performance of the CF-mMIMO network versus the cellular mMIMO deployment. Furthermore, the selected designs from UA1_2 until UA1_5 are composed of MAPs and SAPs (CF-mMIMO heterogenous network). As described in [1], we also consider the possibility to complement a cellular mMIMO network with CF-mMIMO network composed of SAPs. The name attributed to these network designs is suffixed by 'bis'.

The following figures illustrate the selected network designs in UA1.

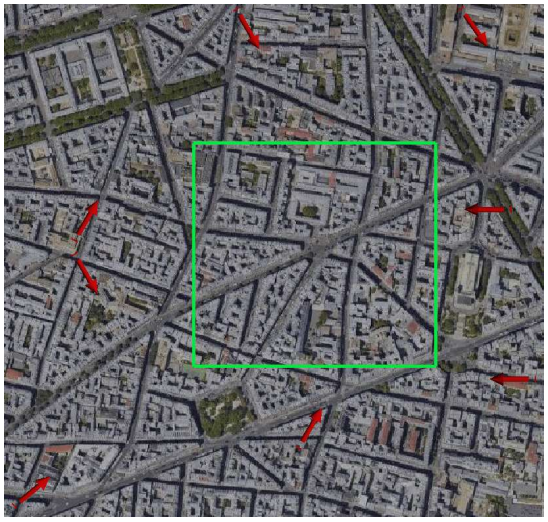

Figure 9 – Network design UA1_1

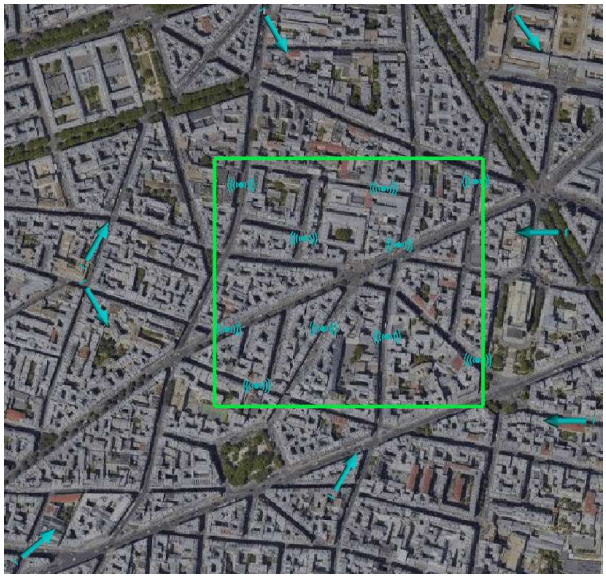

Figure 10 – Network design UA1_2, UA1_2bis

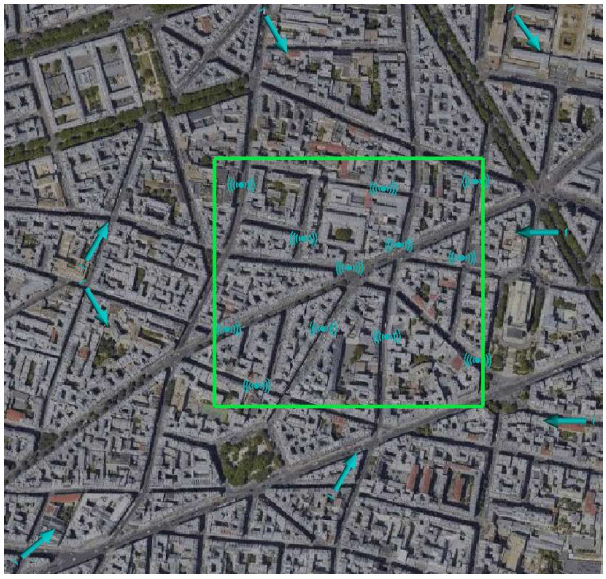

Figure 11 – Network design UA1_3, UA1_3bis

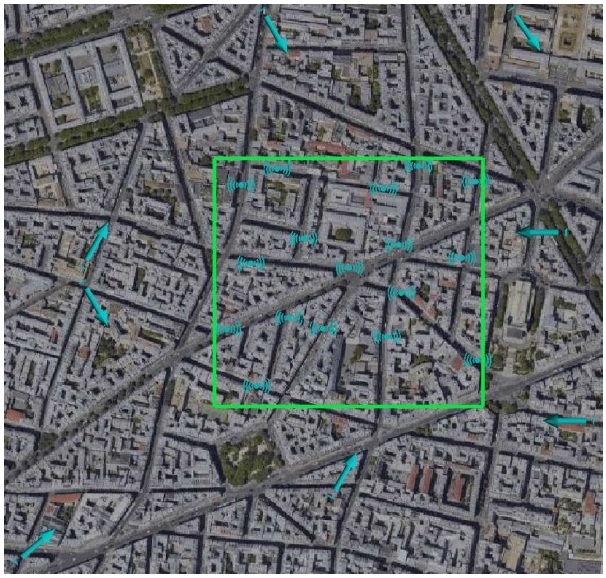

Figure 12 – Network design UA1_4, UA1_4bis

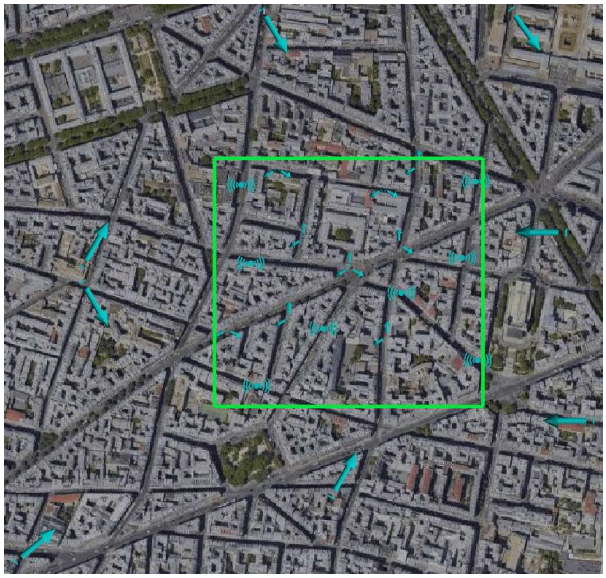

Figure 13 – Network design UA1_5, UA1_5bis

2.1.5.2 UA2 selected designs:

Similarly to UA1, we selected 9 network designs in UA2. Table 4 summarizes the number of APs per design.

Table 4: Summary of selected network designs for UA2

Network design	UA2_1	UA2_2 UA2_2bis	UA2_3 UA2_3bis	UA2_4 UA2_4bis	UA2_5 UA2_5bis
#APs	9 BS	9 BS/MAP+23 SAP omni	9 BS/MAP+28 SAP omni	9 BS/MAP+42 SAP omni	9 BS/MAP+20 SAP omni+57 SAP directive

UA2_1 is a selected design useful for benchmarking purpose. The selected network designs from UA2_2 until UA2_5 are composed of MAPs and SAPs (CF-mMIMO heterogenous network) and the network designs suffixed by 'bis' correspond to the designs composed cellular mMIMO BSs complemented with CF-mMIMO SAPs.

The following figures illustrate the selected network designs in UA2.

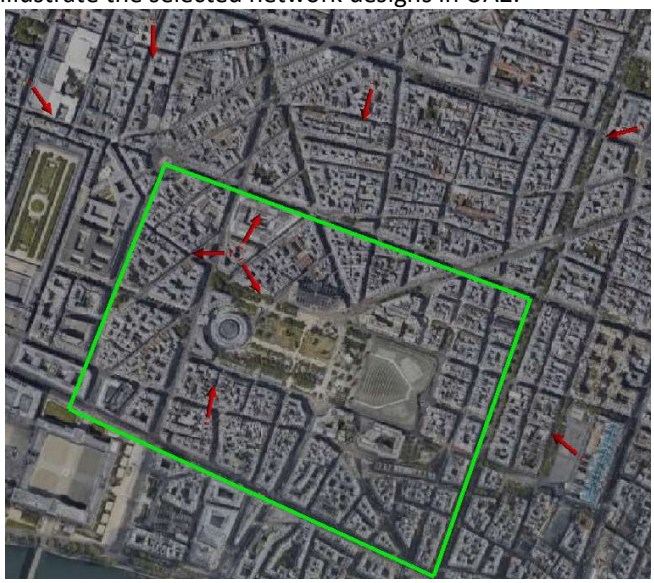

Figure 14 – Network design UA2_1

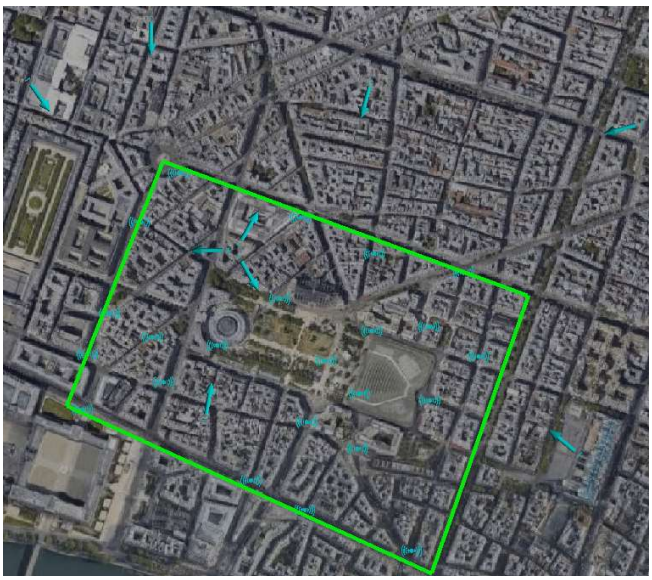

Figure 15 – Network design UA2_2

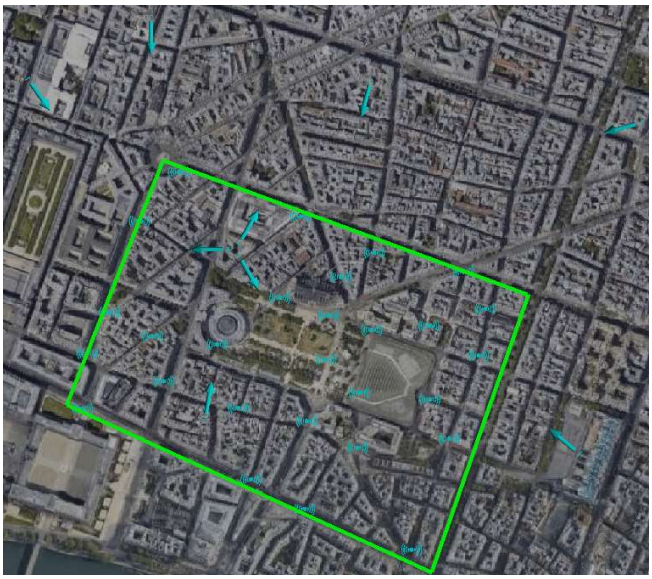

Figure 16 – Network design UA2_3

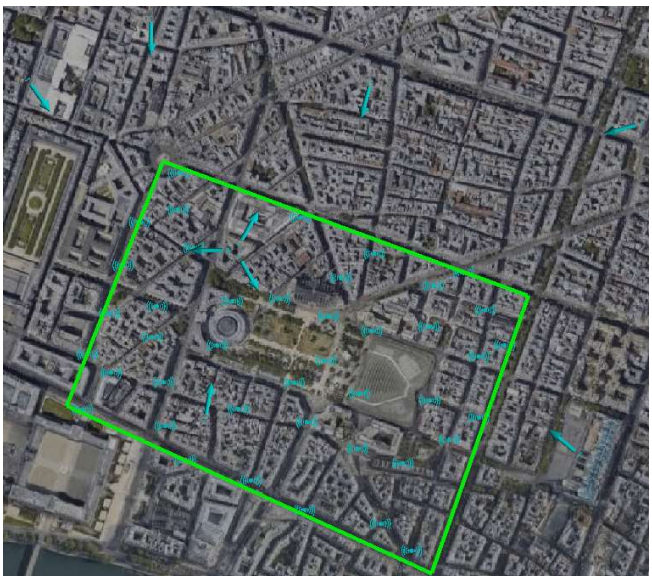

Figure 17 – Network design UA2_4

Figure 18 – Network design UA2_5

2.2 Factory scenarios for private networks

2.2.1 Study areas

Similarly to public networks, we consider two different configurations of the factory area. In the first configuration, we consider an area with few furniture, less obstructed as depicted in Figure 19. However, in the second configuration, we add several obstructing metal racks (see Figure 20).

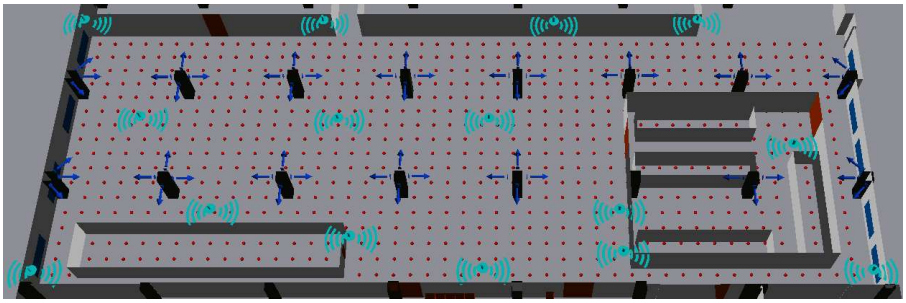

Figure 19 – Study area, network infrastructure (APs candidates) and UEs distribution in FA1

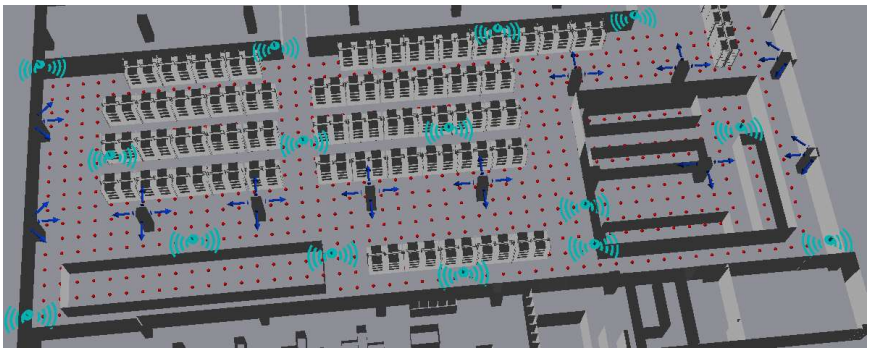

Figure 20 – Study area, network infrastructure (APs candidates) and UEs distribution in FA2

In the rest of the document, we refer to the first configuration as **FA1** for the empty factory space and **FA2** for the second configuration of loaded factory.

2.2.2 Network sites candidates

Channel predictions are made for two different types of SAPs:

- CF-mMIMO omnidirectional SAPs operating at 3.7 GHz: SAPs are placed under the ceiling and 1m away from walls. Therefore, we consider 15 SAPs for both scenario configurations FA1 and FA2.

- CF-mMIMO directive SAPs operating at 3.7 GHz: For directive SAPs, we consider 4 sectors per site installed against the present pillars in the scene. So, we count 53 SAPs distributed over 15 sites in FA1 and 37 SAPs distributed over 11 sites.

Table 5 summarizes the important AP parameters that we consider in the channel predictions.

Table 5: Parameters configuration for private APs

Parameter	Value	
	Omni AP	Directive AP
Spectrum	3.7 GHz / 100 MHz	
	Target frequency resolution = 1 RB	
AP configuration	Height: 4.5-5m Sectorization: directive when placed against pillars; omni when placed under the ceiling Prediction radius: 200m	
AP antenna	128 AEs: 4x4x4x2 Dual-polar (V/H) Cubic array with separation λ/2 Radiation pattern per AE: omni Gain per AE: 6 dBi	128 AEs: 8x8x2 Dual-polar (V/H) Planar vertical antenna array with separation λ/2 Beamwidth per AE: H120°, V60° Gain per AE: 7.8 dBi

2.2.3 Data traffic distribution

In the factory scenario, UEs are uniformly distributed in a grid of resolution 2 m over the study area, which is equivalent to a density of 0.25 UEs/m². In total, we count 850 UEs in FA1 and 756 UEs in FA2 all configured at a height of 1.5 m above the ground.

The UEs parameters including antenna parameters are summarized in Table 6.

Table 6: Parameters configuration for UEs

Parameter	Value
UE configuration	Height: 1.5m Density: 0.25 UE/m²
UE antenna	4 AEs Dual-polar (V/H) 2x1 horizontal linear array with separation λ/2 Radiation pattern per AE: isotropic Gain per AE: 0 dBi

2.2.4 Mobility (machines)

Mobility in the factory is one of important concerns in industry 4.0 use cases. It includes automated guided vehicles (AVG) and forklift trucks (see Figure 21), remote controlled robots…

Similarly to the urban mobility scenarios, we propose two sets of channel data for mobile connected UEs in the factory:

- VF1: Few forklift trucks (around 3) travelling in FA2 for a small period of time (1 second) with resolution of 1 ms.

- VF2: Few forklift trucks (around 3) travelling in FA2 for a longer period of time (60 seconds) with resolution of 100 ms.

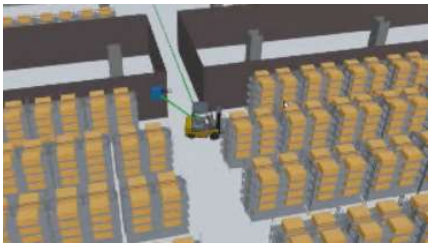

Figure 21 – Illustration of the signal propagation within factory mobility scenarios

2.2.5 Selected network designs

With the considered candidate APs, there can be various possible network designs to be studied. Each researcher/partner in POSEIDON can optimize its algorithms and solutions based a specific design. Nevertheless, we decided to validate our different contributions and evaluate the efficiency of our propositions using a common set of network deployments.

2.2.5.1 FA1 selected designs

For FA1, we selected 5 network designs. We aim to study the impact of variating the APs density and then the use of directive antennas versus omnidirectional ones.

Table 7 summarizes the number of APs per design.

Table 7: Network design summary for FA1

Network design	FA1_1	FA1_2	FA1_3	FA1_4	FA1_5
#APs	3	7	10	10	26
Antenna type	Omnidirectional	Omnidirectional	Omnidirectional	Omnidirectional	Omni + Directive

The following figures illustrate the selected network designs in FA1.

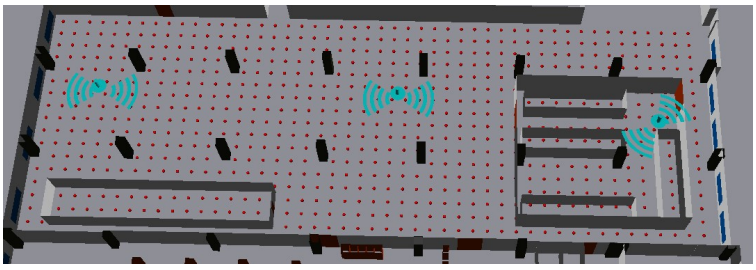

Figure 22 – Network design FA1_1

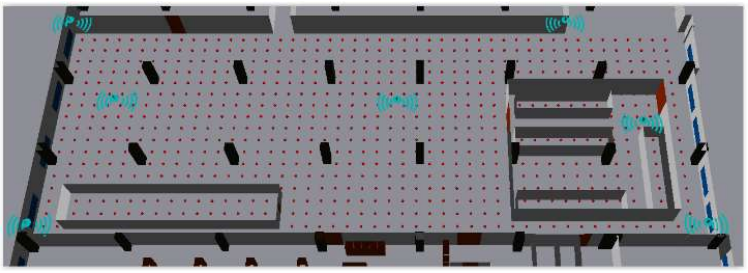

Figure 23 – Network design FA1_2

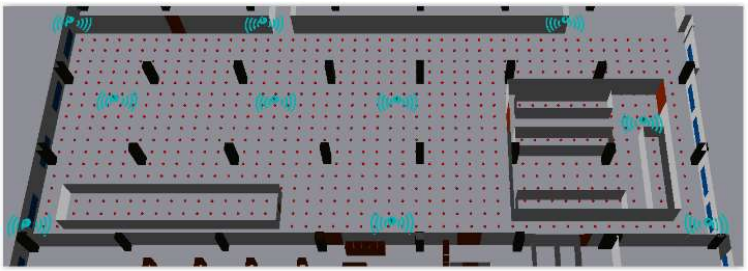

Figure 24 – Network design FA1_3

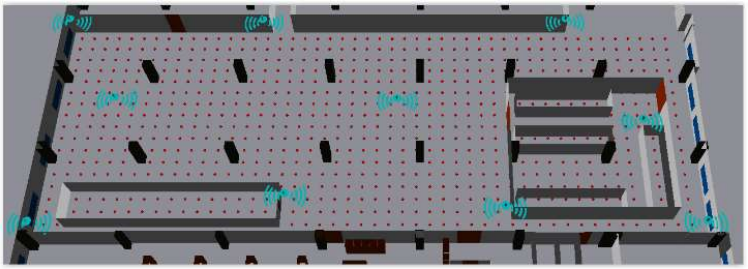

Figure 25 – Network design FA1_4

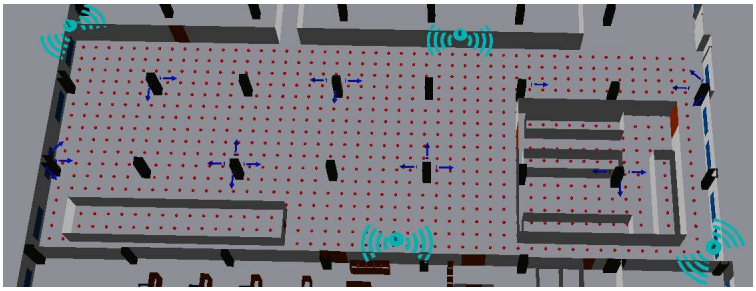

Figure 26 – Network design FA1_5

2.2.5.2 FA2 selected designs

For FA2, we selected 5 network designs. We aim to study the impact of variating the APs density and then the use of directive antennas versus omnidirectional ones. Table 8 summarizes the considered APs per design.

Table 8: Network design summary for FA2

Network design	FA2_1	FA2_2	FA2_3	FA2_4	FA2_5
#APs	4	7	10	23	28
Antenna type	Omnidirectional	Omnidirectional	Omnidirectional	Omni+Directive	Omni+Directive

The following figures illustrate the selected network designs in FA2.

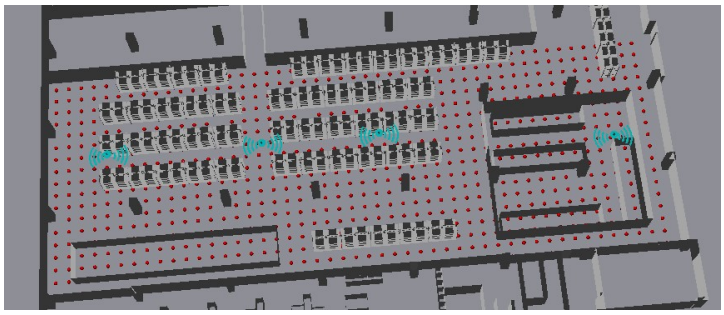

Figure 27 – Network design FA2_1

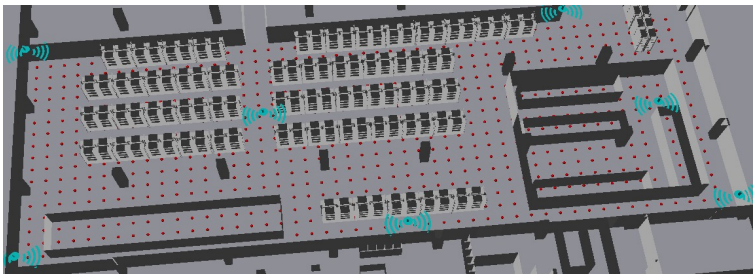

Figure 28 – Network design FA2_2

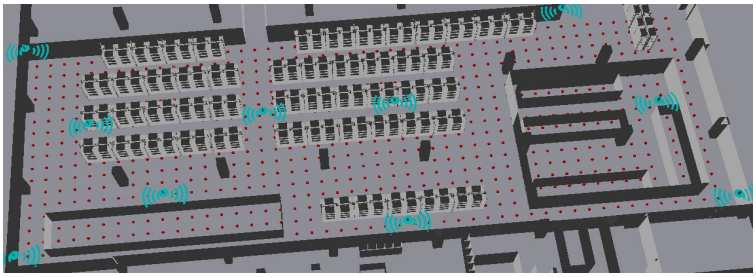

Figure 29 – Network design FA2_3

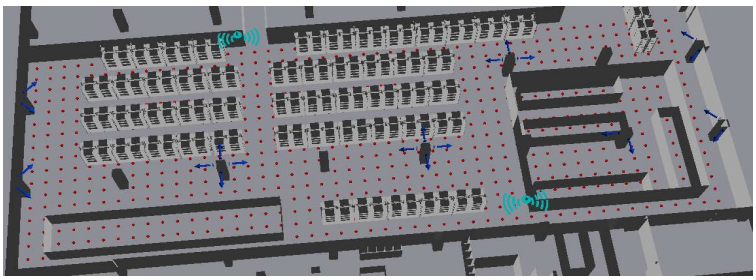

Figure 30 – Network design FA2_4

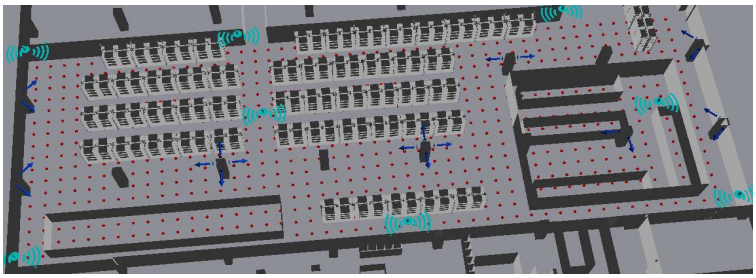

Figure 31 – Network design FA2_5

3 Channel samples database

3.1 Propagation calibration

In general, the potential for depolarization in a channel can be attributed to several factors: 1) the propagation planes are oblique, 2) the surfaces are dielectric, 3) succession of interactions in different places, and 4) scattering phenomena by the surface roughness or the many small objects in the environment. In urban scenarios, the simulated ray depolarization is quite significant due to the capacity of the ray-tracing tool to combine numerous interactions such as building reflection, building edge diffraction and rooftop diffraction; also, a calibration is already embedded in the tool, which was determined from comparison to urban macro-cell dual-polar measurements [4]. Besides, for indoor environments, the ray-tracing configuration results from a necessary trade-off between accuracy and computation times; it is not possible to reproduce all depolarization mechanisms if computation times must be kept reasonable; and there is no pre-defined calibration.

Initially, the in-factory propagation simulation was conducted without any depolarization calibration, resulting in strong isolation between vertical and horizontal propagated polarizations (see Figure 32). To provide more realistic channel samples, we used the same calibration parameters as introduced for the urban model, and adjusted them to align with the 3GPP InF model [5] and dual-polar measurements collected by SIRADEL and CEA-Leti within the ANR project S2LAM (not published yet). The 3GPP model proposes the depolarization to be introduced by a random Cross-Polarization Ratio (XPR) applied independently to each ray, with an average of 12 dB in Line-of-Sight (LOS) and 11 dB in Non-Line-of-Sight (NLOS). The standard deviation is 6 dB. As well, the dual-polar measurements from the S2LAM project indicate an XPR in the range of 10-12 dB.

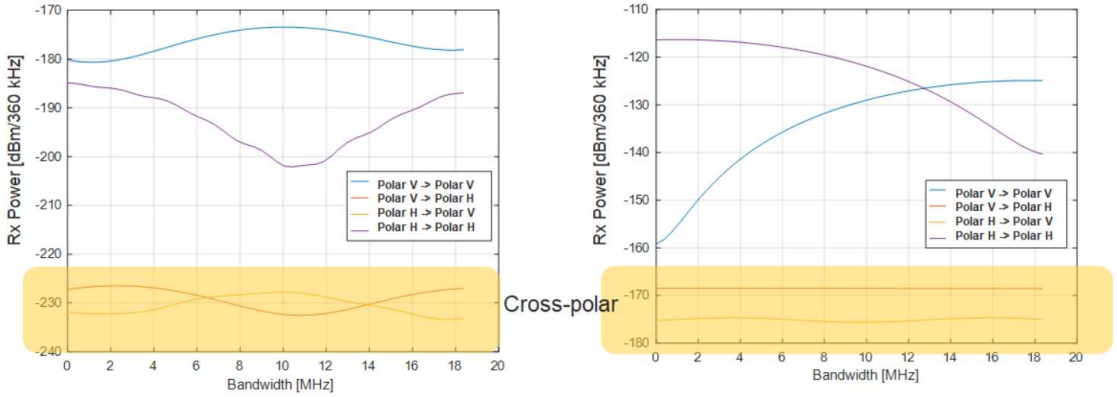

Figure 32 – Frequency channel response level for all polar combinations for 2 links in FA1

The calibration process enabled us to find a balanced solution for both LOS/NLOS links and for both factory scenarios FA1 and FA2. The ratio achieved between the VV and HV polarization terms is summarized in Table 9.

Table 9: Depolarisation performance in terms of VV-VH

	FA1				FA2			
	LOS		NLOS		LOS		NLOS	
	Median	STD	Median	STD	Median	STD	Median	STD
Calibration (few links)	13.8	6.2	9.3	4.1	13.1	7.0	10.2	4.8
Test (all links)	15.5	6.4	11.6	5.5	14.2	6.8	9.5	5.9

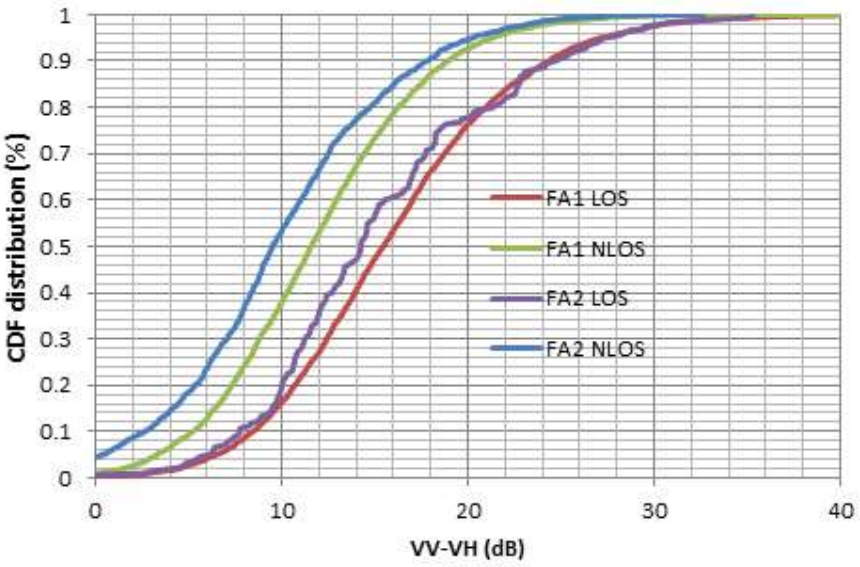

Figure 33 – CDF of the difference between the received power in VV and in VH

Figure 33 shows the CDF of the difference in received power between VV and VH polarizations. The performance achieved demonstrates a satisfactory balance across diverse environments. This includes the two factory scenarios FA1, which mainly consists of LOS links, and FA2, where propagation is significantly obstructed by racks.

3.2 Challenges for storage and exploitation

The four scenarios outlined in the previous section encompass thousands of links between BSs/ APs and UEs. For each link, it is necessary to account for several hundreds of frequency shifts, along with a comprehensive antenna configuration at both the transmitting and receiving ends. As a result, the channel samples database is expected to house several terabytes of data.

The management, storage and utilization of such a vast volume of data can prove to be impractical, particularly when conducting Monte Carlo simulations with varying sets of UEs and for diverse potential network designs. For instance, the user must have access to a robust internet connection and a high-performance computer, primarily with substantial storage capacity. These constraints make straightforward utilization of the database almost unfeasible.

An efficient data compression strategy is crucial to simplify data exploitation, making it quicker and less resource-intensive. This approach will help overcome the limitations and make the process more manageable.

3.3 Data compression

In this section, we present two main compression methods that we analysed during the channel samples data generation phase: i) Evaluate the coherence bandwidth and then reduce the number of frequencies used to generate the channel matrices, ii) Apply a TDL compression.

The compression parametrization and performance (coherence bandwidth, compression rate, RMSE,, Cosine similarity and computation time) are evaluated for 5 different scenario categories, since the results vary with the environment, the propagation range and the antenna directivity:

- Urban Macro network layer: it covers the Cellular mMIMO network in addition to the MAPs in the CF-mMIMO network in the two urban areas UA1 and UA2
- Urban Omni Small network layer: it covers the omnidirectional SAPs in UA1 and UA2
- Urban Directive Small network layer: it covers the directive SAPs in UA1 and UA2
- Factory Omni Small network layer: it covers the omnidirectional SAPs in FA1 and FA2
- Factory Directive Small network layer: it covers the directive SAPs in FA1 and FA2

3.3.1 Coherence bandwidth analysis

The coherence bandwidth is a measure of the frequency spread over which a wireless channel behaves approximately as a flat fading channel.

As explained in Table 1, the signal is formed by 273 RBs (sub channels) in the frequency domain. The objective of the evaluation of the coherence bandwidth is to find the number of RBs over which the channel is almost flat and then reduce the number of frequency-selective MIMO channel coefficients.

In the following analysis, the coherence bandwidth corresponds to the bandwidth size which is valid for 90% of the considered links (with SISO pathloss higher than -170 dB).

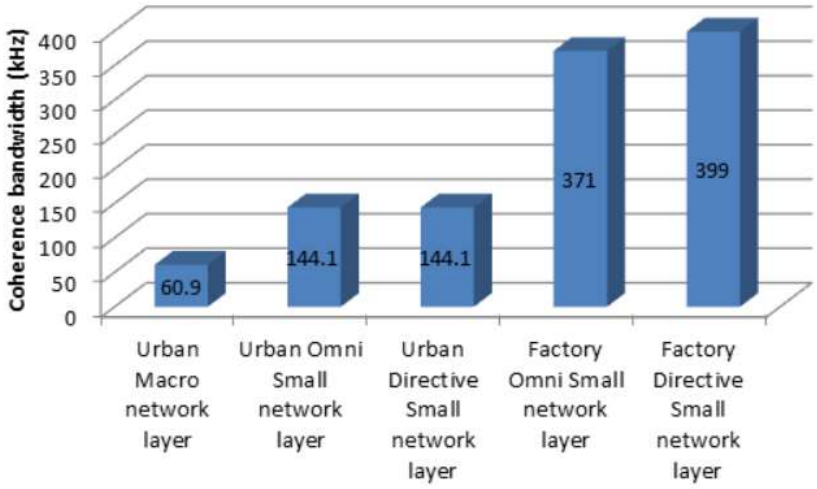

Figure 34 – Coherence bandwidth (kHz)

We observe from Figure 34 that the coherence bandwidth for the Urban Macro network layer is significantly lower compared to the bandwidth of one RB. Consequently, we cannot exploit this method to reduce the data size. So, we decided to explore another approach which consists in multipath clustering.

3.3.2 TDL model

The TDL model [2][6] is a convenient way to represent multipath channels. It is based on rays clustering without sacrificing accuracy when applying the transfer function and computing the frequency channel response.

After clusterization, the channel is represented by a small number of taps, which are characterized by a delay value and a set of MIMO coefficients at the central frequency.

Several algorithms/models were tested and we converged to a solution that helped to obtain a significant compression ratio and reduce the database size from few Terabytes to few tens of GBs. Rays are clustered with the constraint of an RMSE for each link (all over the frequency bandwidth) smaller than 1dB.

Figure 35 shows link examples where we compare the channel frequency response that was either calculated from the TDL representation (few ray clusters) or from the sum of all individual rays.

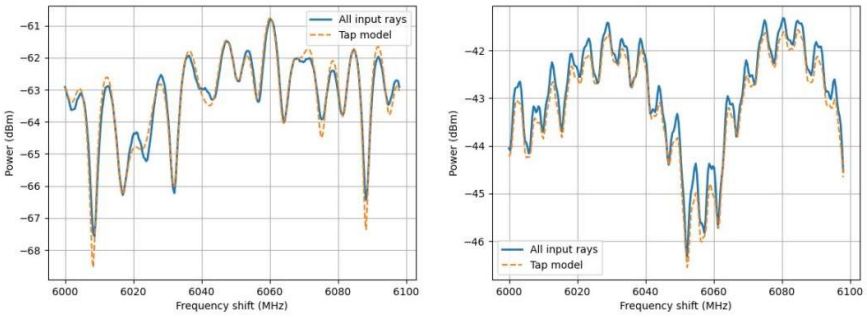

Figure 35 – Channel frequency response for 2 examples of BS-UE link: either derived from TDL representation or all individual rays

3.3.3 Performance analysis

3.3.3.1 Compression rate

We evaluate the performance of the TDL model in terms of compression rate for the different scenarios and configurations based on the following formula:

$$Compression\ rate\ (\%) = 100 \times \frac{Original\ data\ size - Compressed\ data\ size}{Original\ data\ size}$$

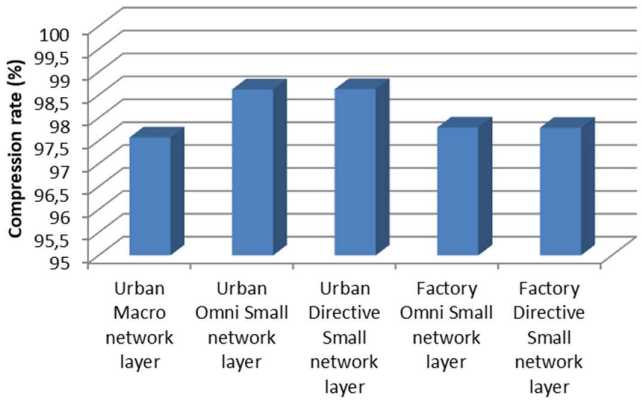

Figure 36 – Compression rate

From Figure 36, we observe that the TDL model shows a very high compression ratio. Consequently, the data size will be significantly reduced which makes the provision and exploitation of the data less complex.

3.3.3.2 Accuracy degradation

Firstly, it is worth noting that it is a common practice to consider logarithmically scaled values and compute the Root Mean Square Error (RMSE) between predictions and measurements when assessing the accuracy of propagation models. Within the context of the POSEIDON project, we did not perform measurements. Instead, we relied on calibrated propagation models derived from previous extensive Siradel studies. The use of the TDL compression introduces a certain level of

degradation compared to full-resolution ray-tracing i.e. with consideration of each individual ray property. However, the degradation versus measurement is necessarily lower. The degradation versus full-resolution ray-tracing, which is reported here below, is an upper bound.

The accuracy of the TDL model is primarily evaluated in terms of RMSE. We also consider an additional metric: Cosine Similarity which evaluates the cosine of the angle between two vectors, providing a good approximation when the cosine similarity is close to 1. These metrics are used in the channel estimation process of wireless communication and can also be utilized to assess channel information compression for communications between the UE and BS/ AP. The RMSE and Cosine similarity are computed using the following formulas:

$$RMSE = \frac{\sum \sqrt{(Predictions_i\,[Log] - Targets_i\,[Log])^2}}{N}$$

$$Cosine\ similarity = \frac{\sum Predictions_i[Lin].Targets_i[Lin]}{\sqrt{\sum (Predictions_i[Lin])^2} \times \sqrt{\sum (Targets_i[Lin])^2}}$$

Where N is the size of the vectors Targets and Predictions.

In terms of RMSE and Cosine similarity, the compression performance is very encouraging as the RMSE is smaller than 1 dB and the cosine similarity is close to 1 (see Figure 37 and Figure 38). This is mainly explained by the fact that the used TDL compression employs an RMSE threshold to find the best taps configuration.

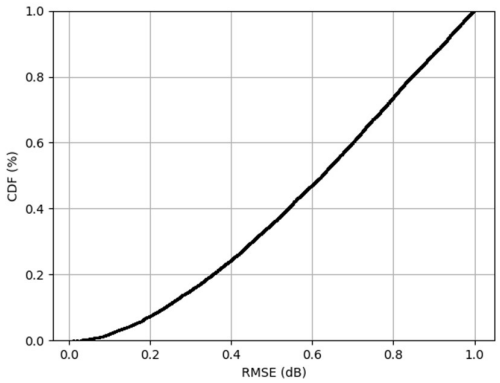

Figure 37 – Accuracy of TDL compression in terms of RMSE

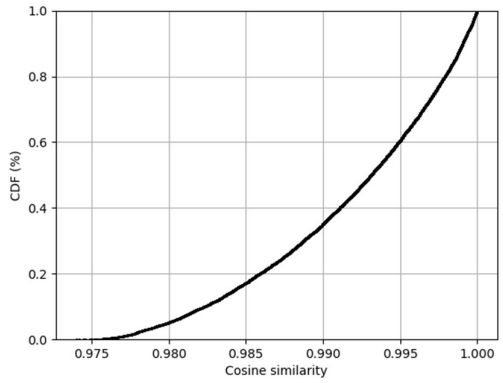

Figure 38 – Accuracy of TDL compression in terms of Cosine similarity

3.3.3.3 Computation time

The computation time is another important factor in the data compression. It is true that the data size is significantly reduced but at the same time, the processing time is increased.

Figure 39 shows the computation time per link, both with and without the application of TDL compression. The results indicate a 130% increase in computation time when TDL compression is applied. Despite this increase, it is considered relatively acceptable because the compression results in a substantial reduction in the data size of the channel samples.

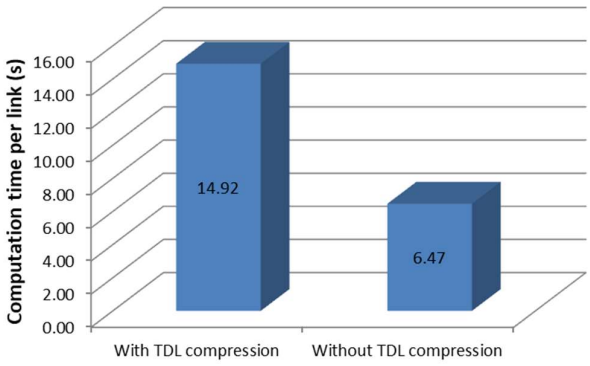

Figure 39 – Additional computation time due to TDL computation

3.4 Description of the channel samples database

The MIMO channel samples are saved in CSV files, which are organized as shown in Figure 40 and Figure 41.

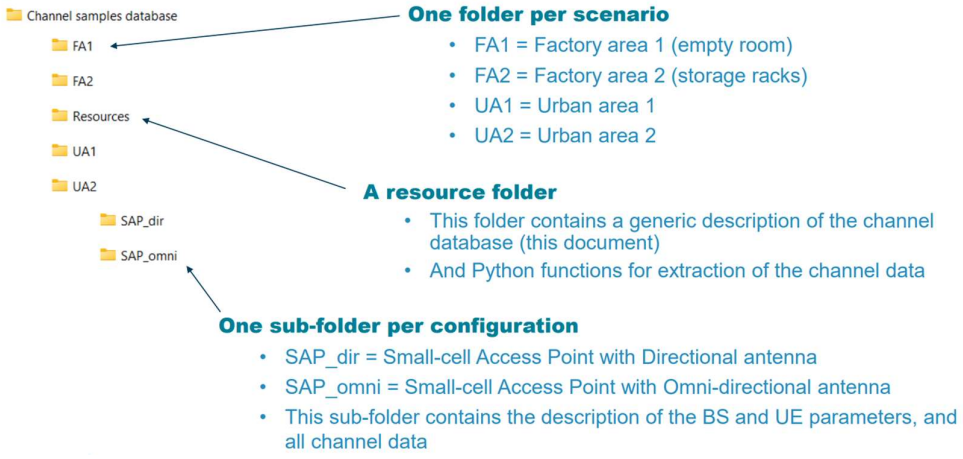

Figure 40 – Channel samples database: folders organization

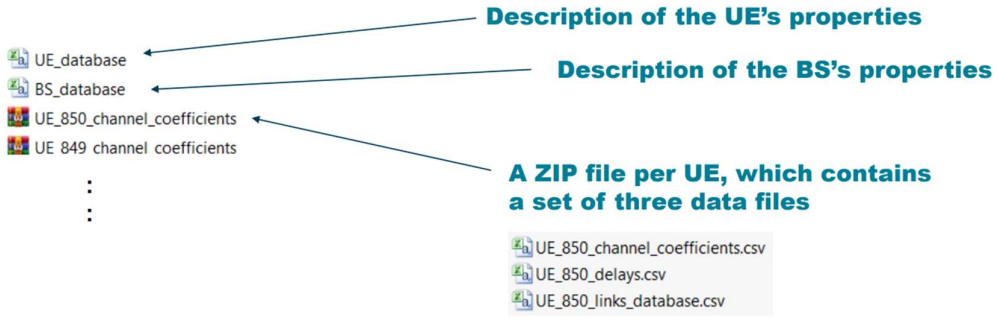

Figure 41 – Channel samples database: files organization in each sub-folder

A detailed description of the channel samples database can be found in Annex A.

3.5 Data extraction

In addition to the channel database, Siradel provides a python script to extract the channel samples corresponding to a specific selection of UEs and BSs/APs and for any desired antenna configuration.

A detailed description of the channel samples extraction and exploitation can be found in Annex B.

4 Preliminary analysis

This section presents a variety of coverage performance metrics and analyses, all of which are resulting from our selected network designs. Our primary objective is to provide an initial, comprehensive overview of the anticipated performance enhancements resulting from network densification, as well as the influence of other network parameters. Our focus is currently centered on factory scenarios. Further analyses, particularly those pertaining to urban scenarios, will be conducted and presented in subsequent deliverables.

As previously detailed in this deliverable, we recall the number of APs per network design below for a more comprehensive analysis of performance metrics under study:

Network design	FA1_1	FA1_2	FA1_3	FA1_4	FA1_5
#APs	3	7	10	10	26
#Sites	3	7	10	10	12
Network design	**FA2_1**	**FA2_2**	**FA2_3**	**FA2_4**	**FA2_5**
#APs	4	7	10	23	28
#Sites	4	7	10	10	16

4.1 Coverage performance: optical visibility

Figure 42 shows the percentage of UEs in LOS with at least one AP (in blue) and to best serving AP (in orange) for both factory scenarios FA1 and FA2 and for the 5 selected network designs.

Note that the best serving AP is defined as the AP with the highest received signal by UEs.

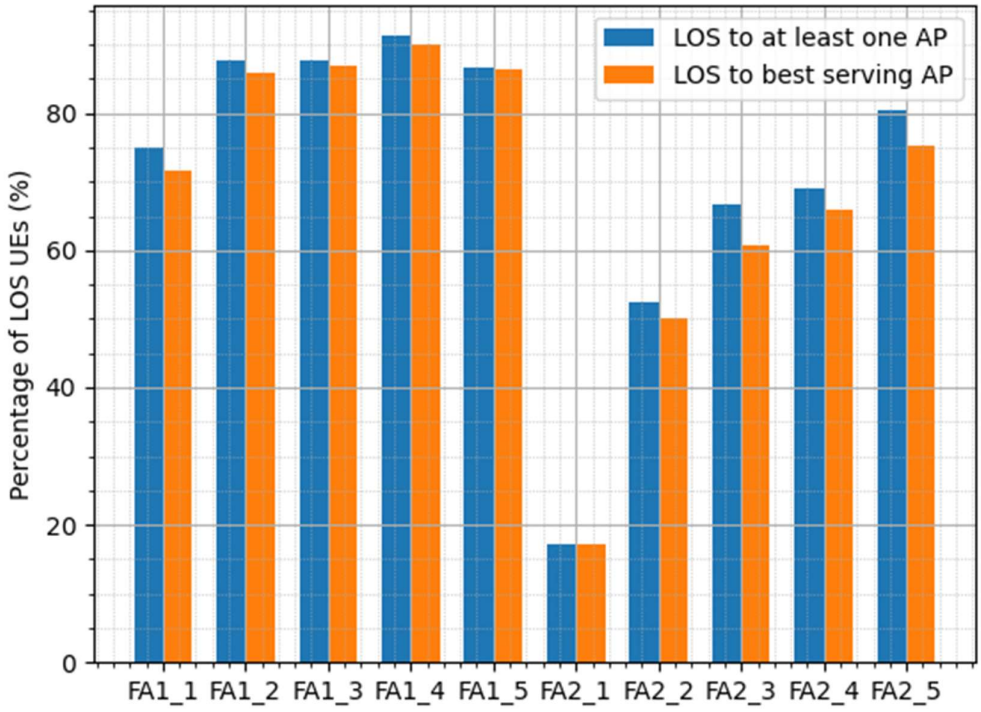

Figure 42 – Distribution of LOS UEs

We observe that in the LOS environment FA1, the percentage of LOS UEs is high since the factory is empty. It slightly increases with the density of APs. However, it slightly decreases when considering

the network design FA1_5 (composed of a mix of omni and directive antennas). For the NLOS environment FA2, we observe that the network densification allows a better LOS coverage as expected. The LOS coverage of the selected design FA2_5 is slightly lower than for FA1_5 despite the obstruction created by the racks in the scenario FA2.

The following table shows the percentage of UEs in LOS with 0 to 6 or more APs:

% UEs							
#LOS APs	0 APs	1 APs	2 APs	3 APs	4 APs	5 APs	≥6 APs
FA1_1	25.06	29.18	45.76	0.00	0.00	0.00	0.00
FA1_2	12.35	12.35	14.94	22.12	25.53	12.47	0.24
FA1_3	12.35	9.88	2.24	6.12	8.82	15.29	45.29
FA1_4	8.71	12.47	3.29	5.41	10.82	16.00	43.29
FA1_5	13.29	2.71	6.71	4.00	1.41	1.41	70.47
FA2_1	82.82	12.59	0.59	4.00	0.00	0.00	0.00
FA2_2	47.53	35.18	7.53	9.29	0.47	0.00	0.00
FA2_3	33.29	39.41	9.53	14.35	2.71	0.71	0.00
FA2_4	31.06	16.35	17.18	6.00	8.94	8.47	12.00
FA2_5	19.65	15.06	14.00	18.59	9.18	10.94	12.59

From the obtained results in the table above, we observe that the network densification allows a significant overlap of LOS APs in FA1. However, in FA2, since the environment is obstructed with racks, there are still a significant proportion of UEs without any LOS AP. Furthermore, the LOS overlapping of 6 and more APs is significantly lower in FA2 as compared to FA1.

4.2 Coverage performance: Received power

In this section, we evaluate the distribution of received power per network design. To elucidate the benefits derived from network densification, we propose an examination of two distinct transmit power models. Initially, we consider a scenario with a constant total transmit power per AP. Subsequently, we contemplate a scenario where the total transmit power for the entire network remains constant. In this case, when the network density increases, the power that can be transmitted per AP correspondingly decreases. This approach allows us to understand the trade-offs between network densification and power distribution among APs.

4.2.1.1 Constant transmit power per AP

The following table summarizes the main parameters considered for this analysis section.

Parameter	Value
AP power (dBm)	23 [7]
RSRP threshold (dBm)	-100/-80 [8]

Figure 43 shows the CDF distribution of RSRP received from the best serving AP to each UE. We observe that the RSRP is improved with the network densification in both scenarios FA1 and FA2.

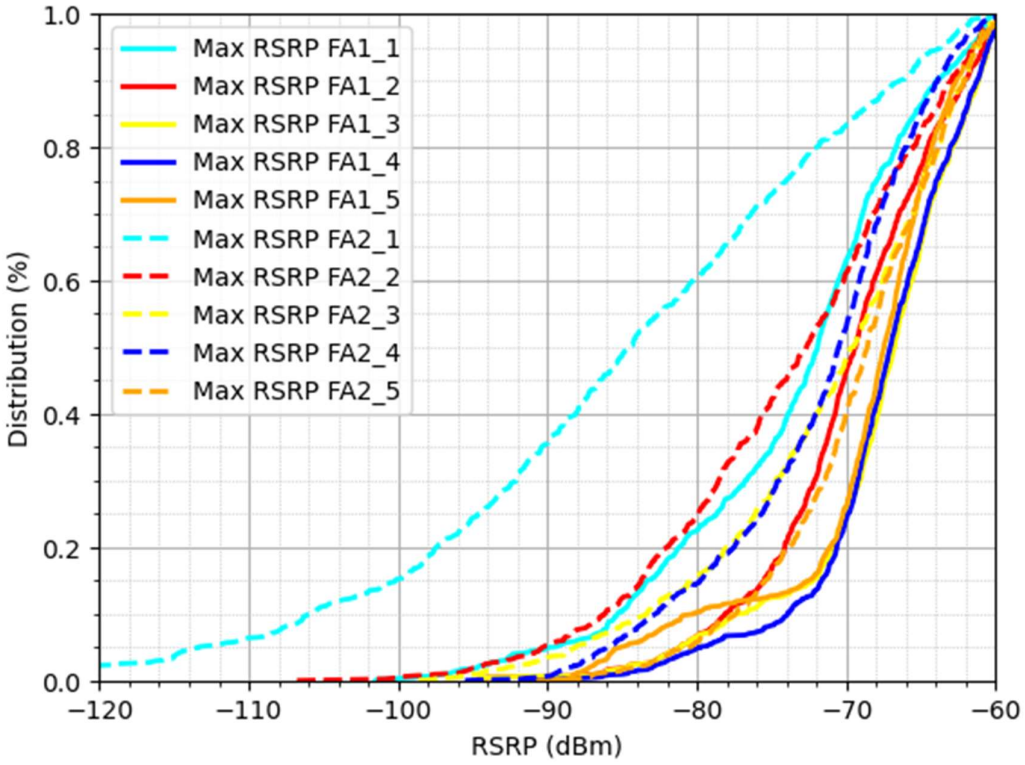

Figure 43 – CDF of RSRP for scenarios FA1 and FA2 for the 5 selected network designs

We evaluate the percentage of covered UEs for each network design in Figure 44**.** Network densification, as anticipated, enhances coverage comprehensively across both scenarios, FA1 and FA2.

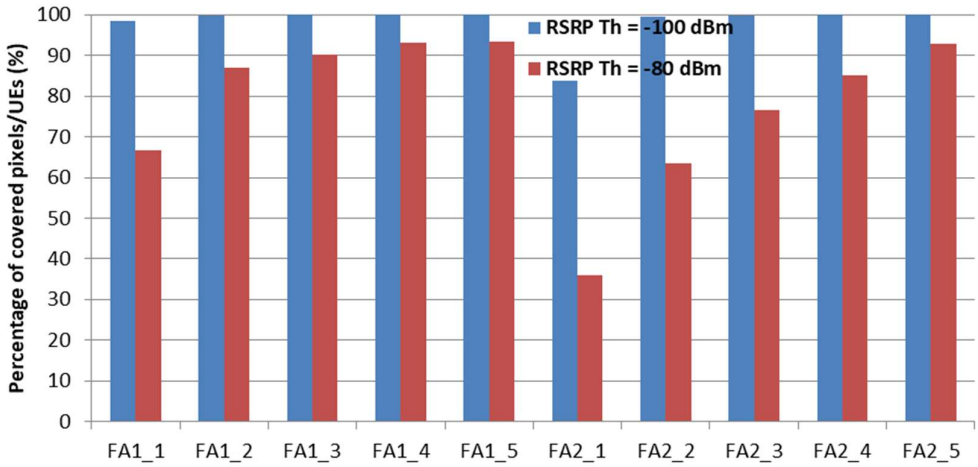

Figure 44 – Distribution of covered UEs

In the following table, we assess the number of detected APs with an RSRP exceeding -100 and -80 dBm respectively, in each UE position. Consistent with earlier findings, the densification of the network facilitates the detection of a greater number of APs. The overlapping gain is enhanced in both scenarios FA1 and FA2 and for both RSRP thresholds. The overlapping gain is significantly reduced with the RSRP threshold of -80 dBm as compared to -100 dBm and specifically in the scenario FA2 since more obstructions are present in the scene. The last two selected network designs (with the highest number of APs) in each of the scenarios FA1 and FA2 respectively cover all the generated UEs with an RSRP higher than -100 dBm. However, around 7% of the UEs cannot be covered with an RSRP higher than -80 dBm.

The typical RSRP thresholds are -80 dBm for excellent signal, between -90 and -80 dBm for good signal, between -100 and -90 dBm for fair signal and between -120 and -100 dBm for poor signal.

	% UEs						
# APs >-100 dBm	0	1	2	3	4	5	≥6
FA1_1	1.65	10.12	20.47	67.76	0.00	0.00	0.00
FA1_2	0.24	4.12	3.65	5.18	6.47	15.65	64.71
FA1_3	0.00	3.06	2.94	2.24	3.18	2.82	85.76
FA1_4	0.00	2.24	2.94	3.53	2.35	2.35	86.59
FA1_5	0.00	0.00	0.47	0.71	0.82	0.82	97.18
FA2_1	16.35	25.65	26.82	31.18	0.00	0.00	0.00
FA2_2	0.59	8.47	16.59	27.76	29.65	15.29	1.65
FA2_3	0.24	4.47	7.76	9.65	15.18	15.29	47.41
FA2_4	0.00	0.35	2.00	2.94	3.29	4.82	86.59
FA2_5	0.00	0.00	0.47	0.94	2.47	2.47	93.65

	% UEs						
# APs >-80 dBm	0	1	2	3	4	5	≥6
FA1_1	33.29	32.35	26.82	7.53	0.00	0.00	0.00
FA1_2	13.18	21.18	24.94	23.06	13.06	4.47	0.12
FA1_3	9.76	11.41	11.41	19.18	19.65	16.94	11.65
FA1_4	6.94	12.35	11.29	21.65	23.76	16.00	8.00
FA1_5	6.71	5.76	4.24	4.12	2.71	2.12	74.35
FA2_1	64.12	26.59	6.35	2.94	0.00	0.00	0.00
FA2_2	36.59	39.18	16.12	7.41	0.71	0.00	0.00
FA2_3	23.53	32.35	22.24	15.41	4.94	1.41	0.12
FA2_4	14.94	20.94	14.35	12.47	11.06	9.65	16.59
FA2_5	7.29	12.00	17.18	18.35	15.18	10.35	19.65

4.2.1.2 Constant transmit power over the network

The following table summarizes the main parameters considered for this analysis section:

Parameter	Value
Total network transmit power (dBm)	23 + 10log(3) = 27.77
RSRP threshold (dBm)	-100/-80

Figure 45 shows the CDF distribution of RSRP received from the best serving AP to each UE. In the FA2 scenario, the densification of the network leads to a marked improvement in the received power. On the other hand, the FA1 scenario shows that allocating constant network power among a smaller number of APs allows a substantial percentage of UEs to attain high received power. Furthermore, the densification of the network fosters more uniform performance, as indicated by the more centralized distribution of the RSRP CDF.

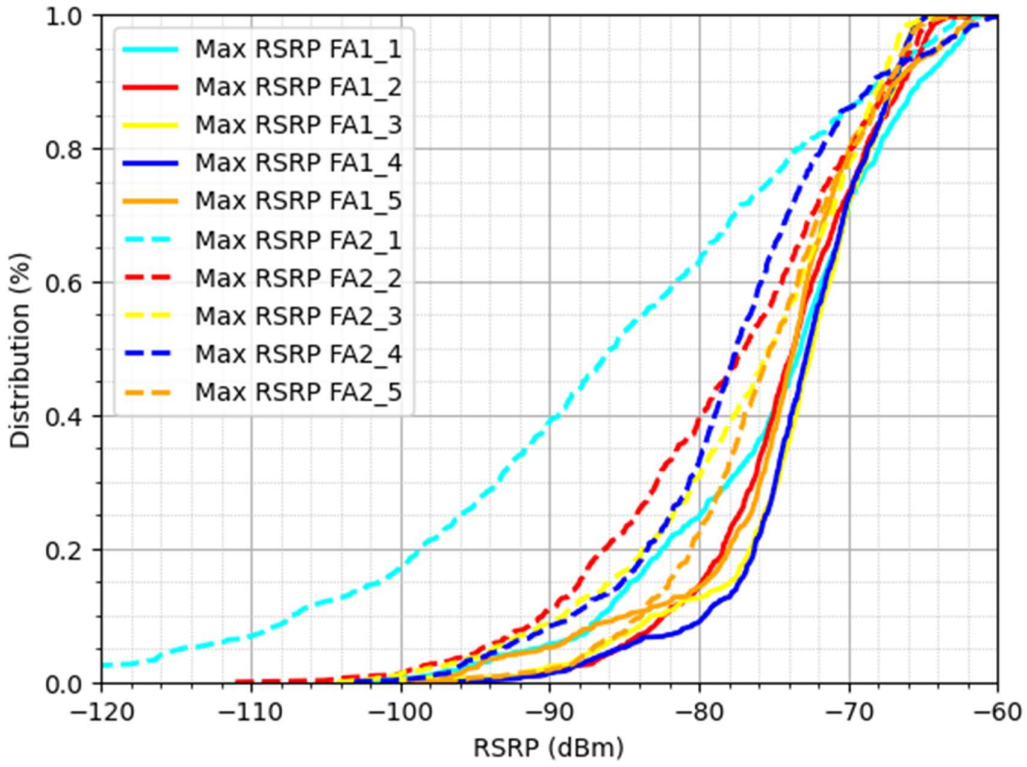

Figure 45 - CDF of RSRP for scenarios FA1 and FA2 for the 5 selected network designs

We evaluate the percentage of covered UEs for each network design in Figure 46**.** The same observations are still valid as in the previous section where the transmit power is constant per AP.

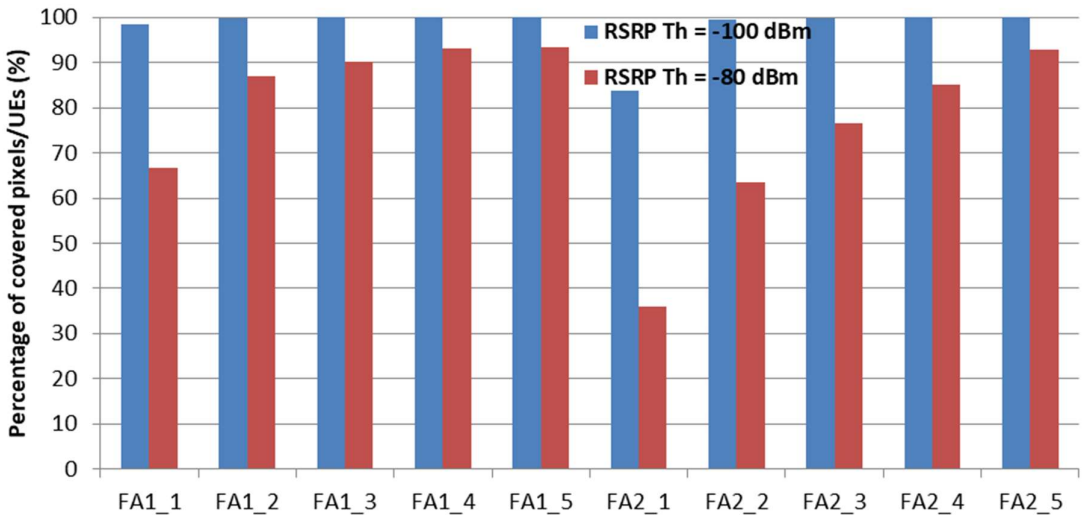

Figure 46 - Distribution of covered UEs

In the following tables, we evaluate the number of detected APs with an RSRP higher than -100 and -80 dBm respectively in each UE position. We observe that considering a constant network power to be shared between different APs leads to improved overlap between APs despite the reduced transmit power per AP. Furthermore, the coverage ratio is not 100% in any of the selected designs in FA1 and FA2 using the RSRP threshold of -100 dBm. Nevertheless, it is almost more than 99% for the last two selected network designs (with the highest number of APs) in each of the scenarios FA1 and FA2 respectively: FA1_4, FA1_5, FA2_4 and FA2_5. In terms of availability and reliability, it is very important to ensure that the most densified selected design covers all the study area with fair signal quality.

	% UEs						
# APs >-100 dBm	0	1	2	3	4	5	≥6
FA1_1	2.35	10.24	23.76	63.65	0.00	0.00	0.00
FA1_2	1.18	6.24	5.18	5.76	9.65	22.71	49.29
FA1_3	1.29	5.18	3.76	3.88	3.53	3.53	78.82
FA1_4	0.12	5.29	4.00	3.18	3.65	4.47	79.29
FA1_5	1.18	1.18	1.29	1.41	2.00	2.35	90.59
FA2_1	19.18	26.59	26.35	27.88	0.00	0.00	0.00
FA2_2	2.47	16.00	23.06	34.24	19.18	4.71	0.35
FA2_3	2.12	11.06	11.53	16.94	19.06	18.12	21.18
FA2_4	0.71	4.94	5.18	6.24	9.41	9.76	63.76
FA2_5	0.47	2.00	1.88	5.06	4.59	6.35	79.65

	% UEs						
# APs >-80 dBm	0	1	2	3	4	5	≥6
FA1_1	37.29	33.53	23.29	5.88	0.00	0.00	0.00
FA1_2	23.76	33.88	26.47	12.71	2.94	0.24	0.00
FA1_3	20.24	26.82	24.94	17.29	8.59	1.88	0.24
FA1_4	17.18	29.41	27.88	17.29	6.82	1.41	0.00
FA1_5	14.82	7.88	11.76	11.88	12.59	12.24	28.82
FA2_1	66.82	25.29	5.76	2.12	0.00	0.00	0.00
FA2_2	51.41	33.41	11.41	3.53	0.24	0.00	0.00
FA2_3	42.12	34.47	16.35	5.65	1.18	0.24	0.00
FA2_4	33.41	32.94	19.29	8.71	3.53	1.53	0.59
FA2_5	22.82	28.71	24.24	15.65	5.41	2.12	1.06

The comprehensive analysis underscores the influence of various network strategies on signal propagation. It provides an initial insight into the potential enhancements that can be derived from network densification. The analysis also reveals the intricacy involved in attaining optimal network performance, particularly when employing directive antennas or maintaining a fixed total transmit power per network. This study serves as a valuable resource for understanding the trade-offs and complexities inherent in the cellular and cell-free mMIMO network optimization.

5 Conclusion

This document offers an in-depth description of four distinct scenarios, the candidate network infrastructure, and the distribution of data traffic across the study areas. For each scenario, we propose five potential network designs. These designs aim to provide a unified basis for all POSEIDON partners to validate methodologies and evaluate performance.

The second part of the document provides a comprehensive overview of the generation extraction, and exploitation of the channel samples database. This process involves the use of TDL compression and propagation calibration.

We then present an initial analysis using the channel samples for the proposed network designs. This analysis primarily focuses on propagation-related metrics, including the distribution of received power, optical visibility, and overlapping indicators.

In the forthcoming deliverables, we will supplement the provided results and analysis with technology-specific metrics, comparing cellular and cell-free mMIMO systems. This will further enhance our understanding and evaluation of the proposed network designs.

6 Bibliography

[1] Jean-Baptiste Doré, David Demmer, Rafik Zayani, Aymen Jaziri, Yoann Corre, Pascal Chevalier, Didier Le Ruyet, Hmaied Shaiek, Amor Nafkha, Haïfa Fares, ‘’Deliverable D1.1: Scenario description KPIs and PHY requirements’’, Sep 2023

[2] Blazek, Thomas, et al. "Vehicular channel models: A system level performance analysis of tapped delay line models." 2017 15th International Conference on ITS Telecommunications (ITST). IEEE, 2017.

[3] Krajzewicz, D., Erdmann, J., Behrisch, M., & Bieker, L. (2012). Recent development and applications of SUMO-Simulation of Urban MObility. International journal on advances in systems and measurements, 5(3&4).

[4] F. Letourneux et al., "Dual-Polarized Channel Measurement and Modeling in Urban Macro- and Small-Cells at 2 GHz," 2017 IEEE Wireless Communications and Networking Conference (WCNC), San Francisco, CA, USA, 2017, pp. 1-6,

[5] 3GPP, “Study on channel model for frequencies from 0.5 to 100 GHz”, TR 38.901 V15.1.0 (2019-09).

[6] 3GPP, “Study on channel model for frequency spectrum above 6 GHz”, TR 38.900 version 14.2.0 (2017-06).

[7] NGO, Hien Quoc, ASHIKHMIN, Alexei, YANG, Hong, et al. “Cell-free massive MIMO versus small cells”, IEEE Transactions on Wireless Communications, 2017, vol. 16, no 3, p. 1834-1850.

[8] NGMN, “Definition of the Testing Framework for the NGMN 5G Trial and Testing Initiative Phase 2”, V 1.8, 2022.